Thermal scattering libraries for cold and very-cold neutron reflector materials

Douglas D. DiJulio[1,*], *Jose Ignacio* Marquez Damian[1], *Marco* Bernasconi[2], *Davide* Campi[2], *Giuseppe* Gorini[2], *Thomas* Kittelmann[1], *Esben* Klinkby[3], *Gunter* Muhrer[1], *Kemal* Ramic[1], *Nicola* Rizzi[3], and *Valentina* Santoro[1]

[1]European Spallation Source ESS ERIC, SE-221 00 Lund, Sweden
[2]University of Milano-Bicocca, Milano, Italy
[3]DTU Physics, Technical University of Denmark

Abstract. We present recent developments of improved modelling methods for simulating neutron transport in reflector materials of interest for neutron source applications. These include materials to be used as traditional reflectors around the neutron moderator, such as beryllium, and also novel materials, such as nanodiamond particles, to be used as a reflector for very-cold neutrons in the neutron beam extraction area of a neutron scattering instrument. Of particular interest is the inclusion of physical effects that are not modelled in standard thermal scattering libraries used for Monte-Carlo simulations, such as extinction in beryllium reflectors and effects of small-angle neutron scattering from nanodiamond particles.

1 Introduction

Reflectors play an important role at reactor and spallation neutron sources, providing a means for otherwise lost neutrons to be potentially re-directed towards the neutron science instruments. Such materials typically surround the moderating volume, such as beryllium, but can also be placed in the neutron beam extraction area in a similar way as a neutron guide, as has been proposed for nanodiamond particles [1]. The standard approach for designing such systems is to perform detailed Monte-Carlo simulations using thermal scattering libraries, which are derived from the microscopic properties of the specific material systems, as input. The models used to generate such libraries do not typically account for macroscopic effects of the materials, such as a finite particle size or texture, and do not include physics beyond simple coherent/incoherent elastic and inelastic scattering. However, some effects, such as extinction [2] due to finite crystallite sizes, can lead to a reduction of the coherent neutron scattering cross-section, which may translate into a reduced performance of a reflector at a neutron source. In the case of nanodiamond particles [1, 3], small-angle neutron scattering is the dominant mechanism for very-cold neutron transport and must be included for a proper description of the scattering process. Cold and very-cold neutrons can be loosely defined to have wavelengths between 2-20 Å and 10-120 Å, respectively [4].

For these reasons, we have launched several different studies to address such challenges. We make use of recent advancements in neutron scattering software, such as NCrystal [5] and NJOY+NCrystal [6], in order to include new physics into the Monte-Carlo simulation process. In the following, we present some examples of these developments, in particular here we focus on the crystallite effects in a traditional beryllium reflector and finite-size effects of nanodiamond particles on the neutron scattering cross-sections. Related work on other reflector materials, such as magnesium hydride, can be found in [6].

*e-mail: douglas.dijulio@ess.eu

2 Beryllium with extinction effects

Standard thermal neutron library generation codes, such as NJOY [7], calculate the coherent elastic cross-section under the powder-average approximation, given by

$$\sigma_{el}^{coh}(\lambda) = \frac{\lambda^2}{2V} \sum_{hkl} d_{hkl} |F_{hkk}|^2, \quad (1)$$

where d_{hkl} is the lattice plane spacing, V is the crystal unit cell volume, λ is the wavelength, hkl are the Miller indices, and F_{hkl} is the structure factor. In reality, however, macroscopic effects, such as finite crystallite size or preferred orientation, lead to deviations from the powder approximation. For example, a finite crystallite size could lead to reduction of the coherent elastic cross-section due to primary extinction [8], while preferred orientation could lead to differences in the cross-section which are dependent on the orientation of the material with respect to the neutrons direction in flight [9].

To explore these effects in more detail, in an earlier paper we reported on an implementation of primary extinction into the thermal scattering library generation process [2, 10] and used the libraries to investigate the impact on the cold moderator brightness at the European Spallation Source (ESS) [11]. The study was inspired from work on neutron Bragg-edge imaging [9]. In this case we investigated the effect due to finite crystallite size, however,

© The Authors, published by EDP Sciences. This is an open access article distributed under the terms of the Creative Commons Attribution License 4.0 (https://creativecommons.org/licenses/by/4.0/).

other effects, such as secondary extinction [12] and preferred orientation can also play a role. The extension of Eq. (1) to include primary extinction is given by

$$\sigma_{el}^{coh}(\lambda) = \frac{\lambda^2}{2V} \sum_{hkl} d_{hkl} |F_{hkk}|^2 E_{hkl}(\lambda, F_{hkl}), \qquad (2)$$

where $E_{hkl}(\lambda, F_{hkl})$ is the extinction factor, which depends on the crystallite size parameter S and more details can be found in [2].

The work presented here is an update to the previous implementation, which has been ported over to the latest version of NJOY+NCrystal. This included a correction to fix an overestimation of the crystallite effect on the coherent scattering cross-section. Additionally, as the ACE format stores the Bragg-edge positions and their magnitudes, during a Monte-Carlo simulation, with MCNP6 [13] for instance, the cross-section between the Bragg edges is extrapolated as $1/E$ as given in Eq. (1). This results in a deviation of the cross-section, calculated by Eq. (2), between the Bragg edges. For the purpose of this work, we have adjusted the magnitude of the Bragg edges by the average difference in the cross-section predicted by Eq. (2) and that predicted by a $1/E$ behavior. A more rigorous approach would require modifications to the Monte-Carlo software.

As a test of the implementation, we found data on BeO from [14]. They measured neutron cross-sections for several BeO samples and reported reduced total cross-sections, compared to predictions from a perfect sample. An interesting finding was that they reported little difference between the neutron cross-sections when measuring across different orientations, leading to the conclusion that the effects they saw could be caused by finite grain sizes.

Figure 1 shows calculations of our implementation in NCrystal with the experimental data from [14]. The crystallite size parameter was adjusted to give approximate agreement with the experimental data. Overall it can be seen that a larger grain size correlates with a larger crystallite size and the general decreasing cross-section as a function of crystallite size is observed.

We received candidate beryllium reflector samples, where the average grain size was characterized to be around 10 microns. Thus we produced libraries at several different crystallite sizes around this value and the scattering cross-sections are shown in Figure 2. These libraries were used in the model described in [2] to estimate the impact on the cold brightness of the ESS moderator system and the average results over the 42 beamports of the ESS are given in Table 1.

Table 1. Average effect due to cystallite size on the performance of the cold moderators at ESS, compared to a perfect reflector.

Crystallite size	Average relative effect
5 microns	99.5%
10 microns	98.5%
15 microns	97.3%

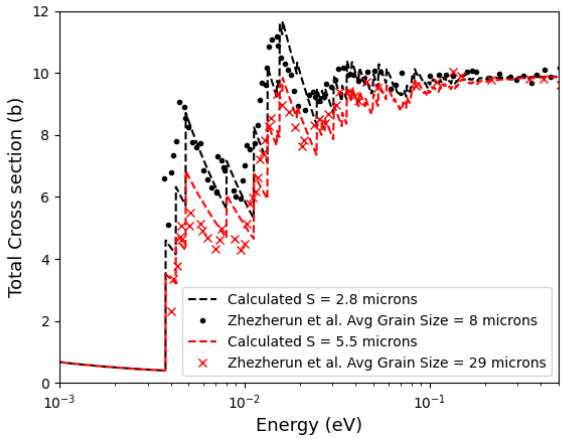

Figure 1. Calculated cross-sections for BeO for different crystallite sizes, compared to digitized data from Fig. 7 of [14]. An additional correction was made to the data to match the cross-sections in the eV energy range.

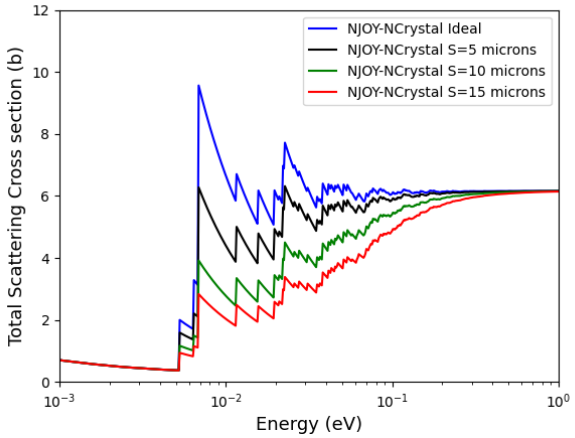

Figure 2. Calculated cross-sections from NJOY-NCrystal for Be as a function of crystallite size.

3 Nanodiamond particles

In earlier works [4, 15] we developed a small-angle neutron scattering component for NCrystal, using its plugin feature, to properly model the complete neutron scattering process. A main ingredient for this model is the phonon frequency distribution, which can be impacted by the finite size of the nanodiamond particles. To investigate this further, we carried out molecular dynamics simulations using a Gaussian Approximation Potential (GAP) [16], where the initial configurations were built using the Wulff construction method. Preliminary results for 5.0 nm nanodiamonds are shown Figure 3, compared to data from [17]. More details and additional calculations will be the topic of a forthcoming paper.

The calculated phonon frequency distribution was used as input to the NCrystal plugin and the scattering cross-sections and components are shown in Figure 4. The

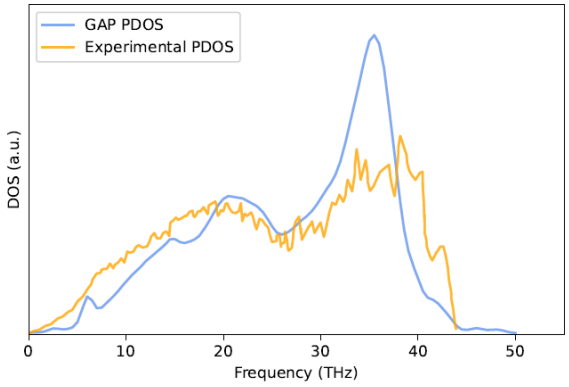

Figure 3. Comparison of the calculated phonon frequency distribution for the 5.0 nm nanodiamond particles to data from [17].

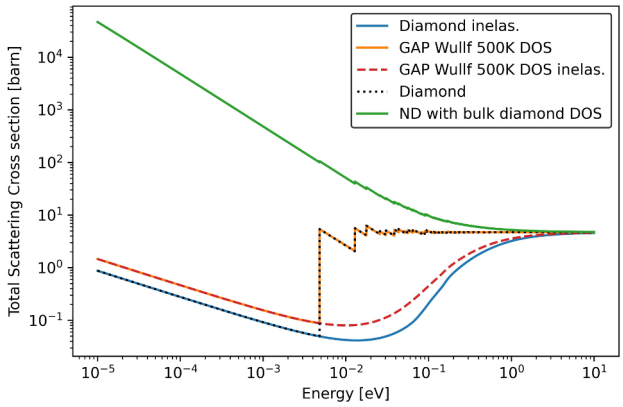

Figure 4. Calculated scattering cross-sections and components for nanodiamonds using the phonon frequency distribution of perfect diamond and the phonon frequency spectrum based on a finite-size of the nanodiamond particles.

results are compared to calculations using the phonon frequency distribution for perfect diamond. From the figure it is seen that the scattering cross-section is dominated by small-angle neutron scattering, while the finite size of the nanodiamonds impacts the inelastic component of the cross-section.

4 Conclusions

In summary, we have presented results of improved modelling techniques of thermal neutron scattering in reflector materials of interest to neutron source facilities. We have focused on implementations of physics that are not traditionally included in the library generation process, such as extinction in beryllium reflectors, due to finite crystallite size, and also small-angle neutron scattering in nanodiamonds, including finite particle-size effects. Continuous work is ongoing related to both current and future moderator systems at the ESS.

Acknowledgements

Part of this work was funded by the HighNESS project at the European Spallation Source. HighNESS is funded by the European Framework for Research and Innovation Horizon 2020, under grant agreement 951782.

References

[1] V. Santoro et al., Journal of Neutron Research 22 (2020) 209-219
[2] D.D. DiJulio et al., Journal of Neutron Research 22 (2020) 275-279
[3] V. Nesvizhevsky et al., Carbon 130 (2018) 799-805
[4] V. Santoro et al., "DEVELOPMENT OF A HIGH INTENSITY NEUTRON SOURCE AT THE EUROPEAN SPALLATION SOURCE: THE HIGHNESS PROJECT", 14th International Topical Meeting on Nuclear Applications of Accelerators, November 30 to December 4, 2021, Washington, DC
[5] X.X. Cai and T. Kittelmann, Comput. Phys. Comm. 246 (2020) 106851
[6] K. Ramic et al., Nuclear Inst. and Methods in Physics Research A 1027 (2022) 166227
[7] R.E. MacFarlane and A.C. Kahler, Nuclear Data Sheets 111 (2010) 2739
[8] T.M. Sabine, Aust. J. Phys 38 (1985) 507
[9] H. Sato, T. Kamiyama and Y. Kiyanagi, Materials Transactions 52 (2011) 1294
[10] Jose Ignacio Marquez Damian et al., Journal of Neutron Research 23 (2021) 157–166
[11] R. Garoby et al., Phys. Scr. 93 (2018) 014001
[12] Dessieux et al., Rev. Sci. Instrum. 89 (2018) 025103
[13] C. J. Werner, et al., "MCNP6.2 Release Notes", Los Alamos National Laboratory, report LA-UR-18-20808 (2018).
[14] I.F. Zherzherun et al., Atomnaya Energiya 13 (1962) 250-257
[15] Ramic et al., Advances in nuclear data and software development for the HighNESS Project, 14th International Topical Meeting on Nuclear Applications of Accelerators, November 30 to December 4, 2021, Washington, DC
[16] P. Rowe, V. L. Deringer, P. Gasparotto, and G. J. Csany, Chem. Phys. 153 (2020) 034702
[17] A. A. Shiryaev et al., Phys. Chem. Chem. Phys. 22 (2020) 13261